

Modelling microstructural alterations under rolling contact fatigue and design of fatigue resistant bearing steels

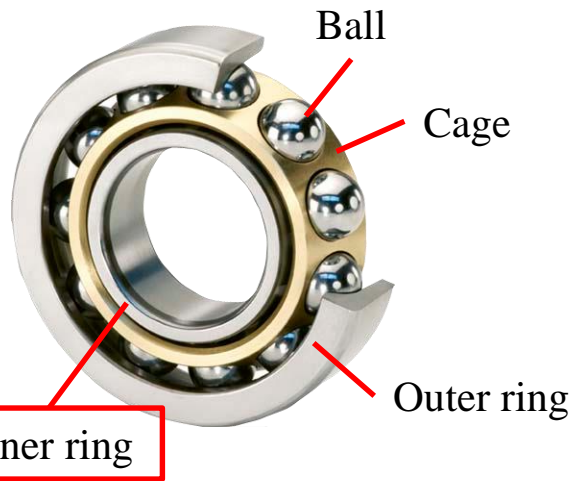
Hanwei Fu*, Enrique Galindo-Nava, Wenwen Song

Supervisor: Pedro Rivera*

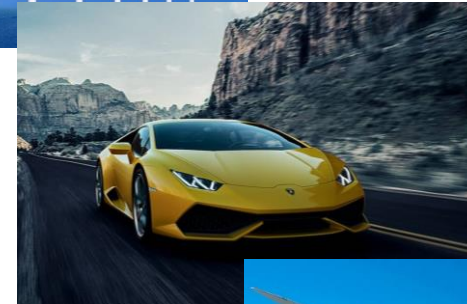
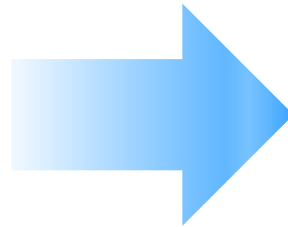
*Department of Engineering, Lancaster University

Rolling contact fatigue (RCF) of bearings

Ball bearing



Applications



Flaking on bearing inner ring

Detrimental service environment:

- High contact pressure (p_0)
- High rotational speed (\dot{N})
- High temperature (T)
- High number of stress cycles (N)

Bearings need to undergo $10^6 - 10^9$ cycles!

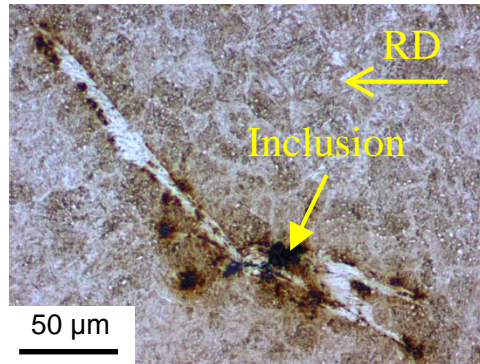
Microstructural alterations under RCF

Three major types of microstructural alterations in bearing steels under rolling contact fatigue (revealed by 2% natal)

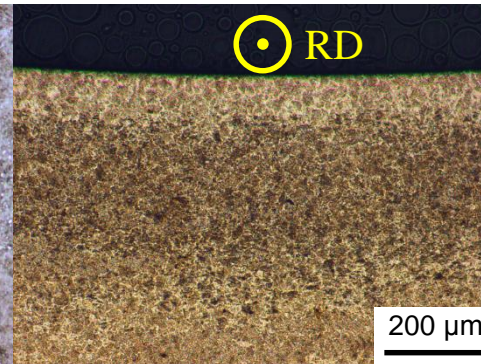
White etching areas (WEAs)

Dark etching regions (DER)

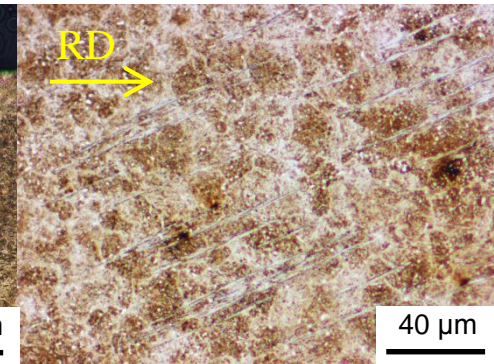
White etching bands (WEBs)



$10^5 - 10^6$ cycles



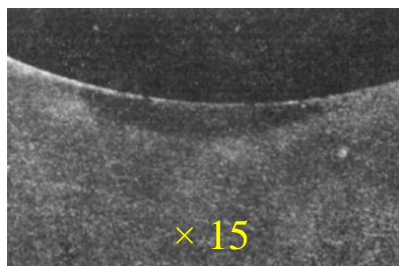
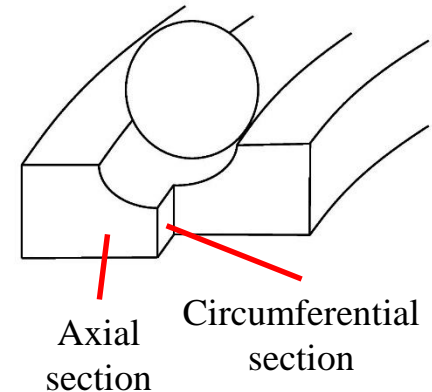
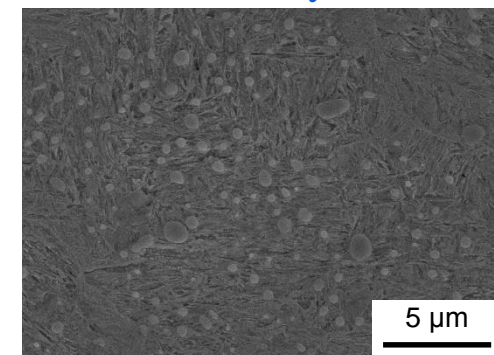
$10^7 - 10^8$ cycles



$10^8 - 10^9$ cycles

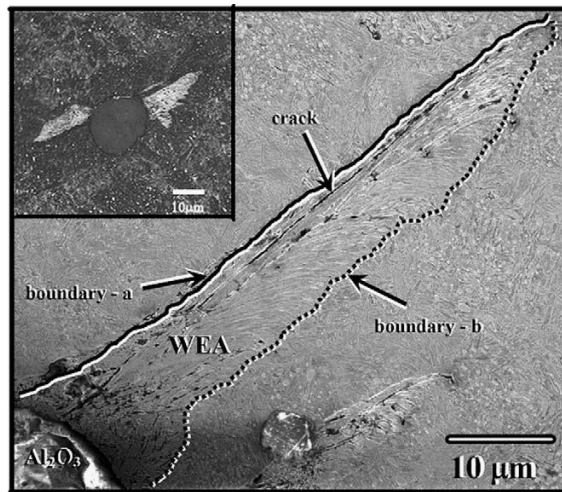
- These microstructural alterations all display martensite decay and alter the mechanical properties of the material.

Initial microstructure: tempered martensite

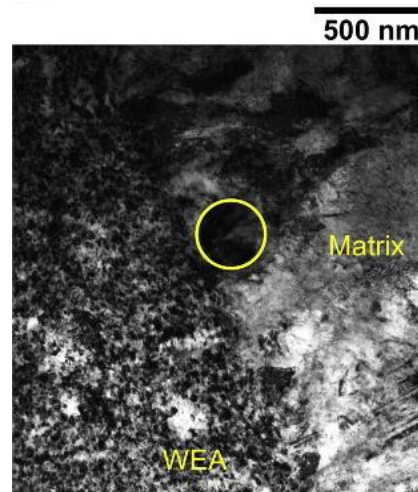


First report in history:
Jones, 1947

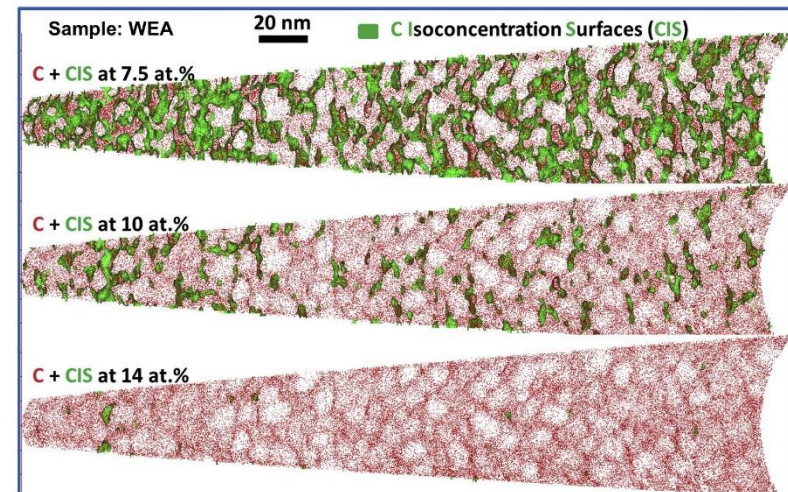
Characterisation – WEAs



Grabulov *et al.*, 2009



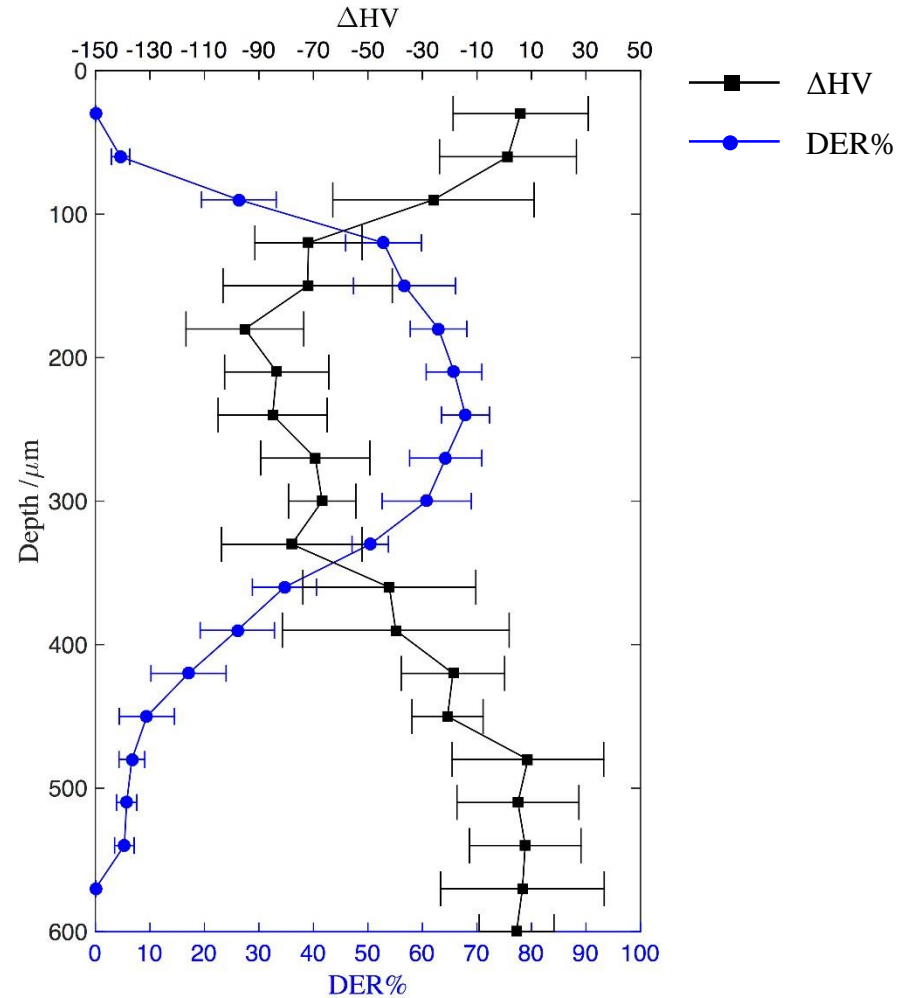
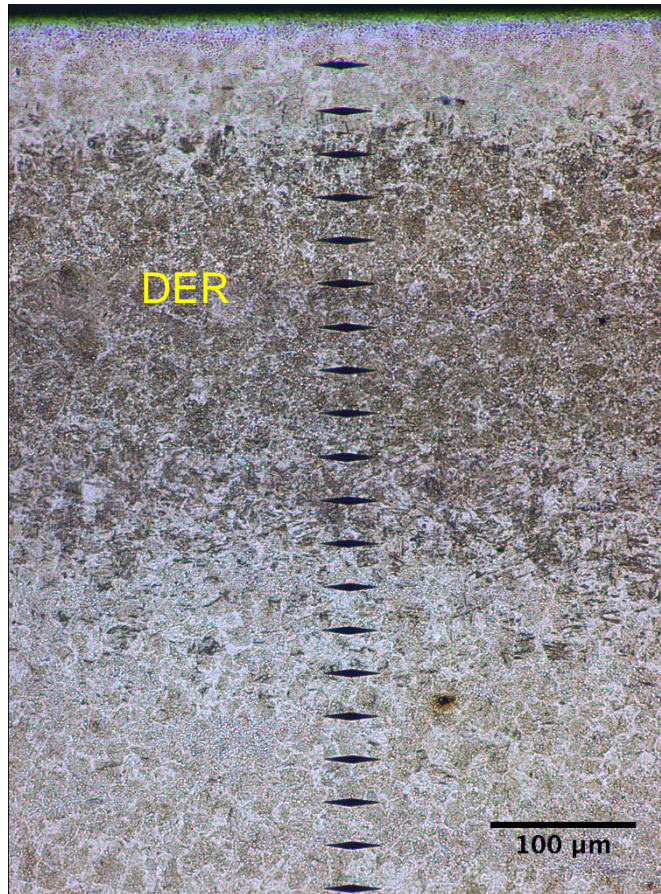
Kang *et al.*, 2013



Li *et al.*, 2014

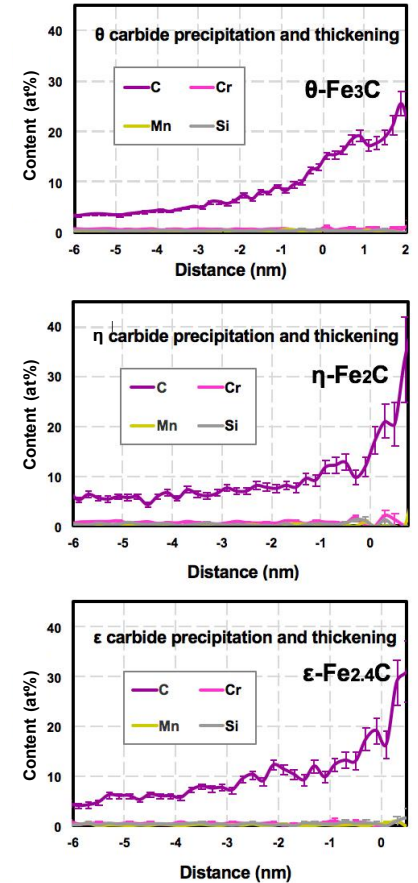
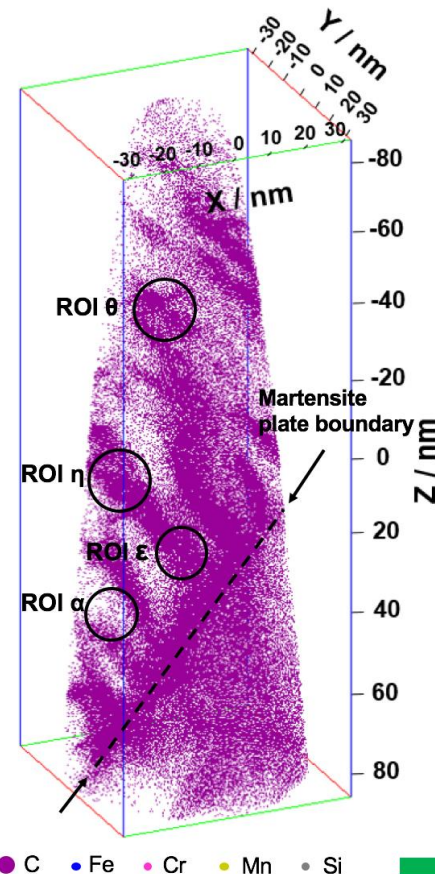
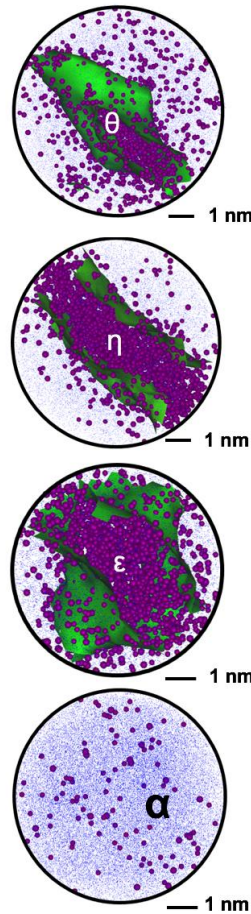
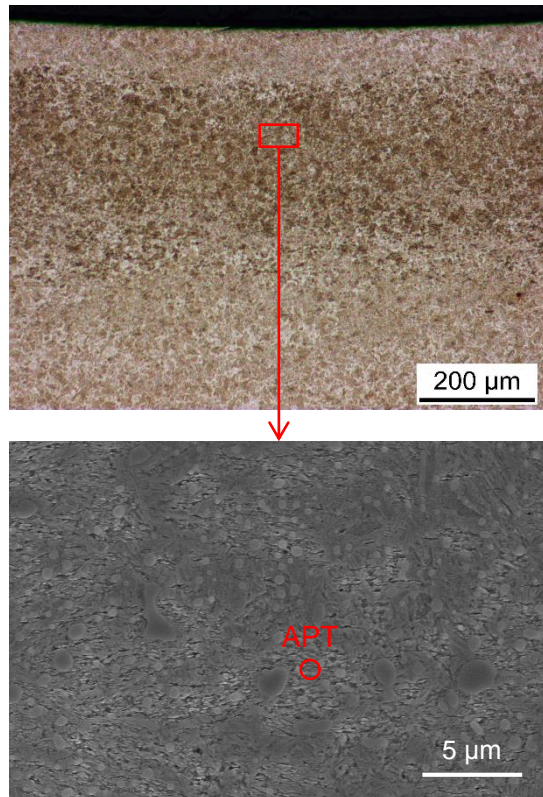
- WEAs consist of nano-sized dislocation cells.
- Carbide dissolution is found inside WEAs.
- **Distinct carbon segregation to cell walls is detected.**

Characterisation – DERs



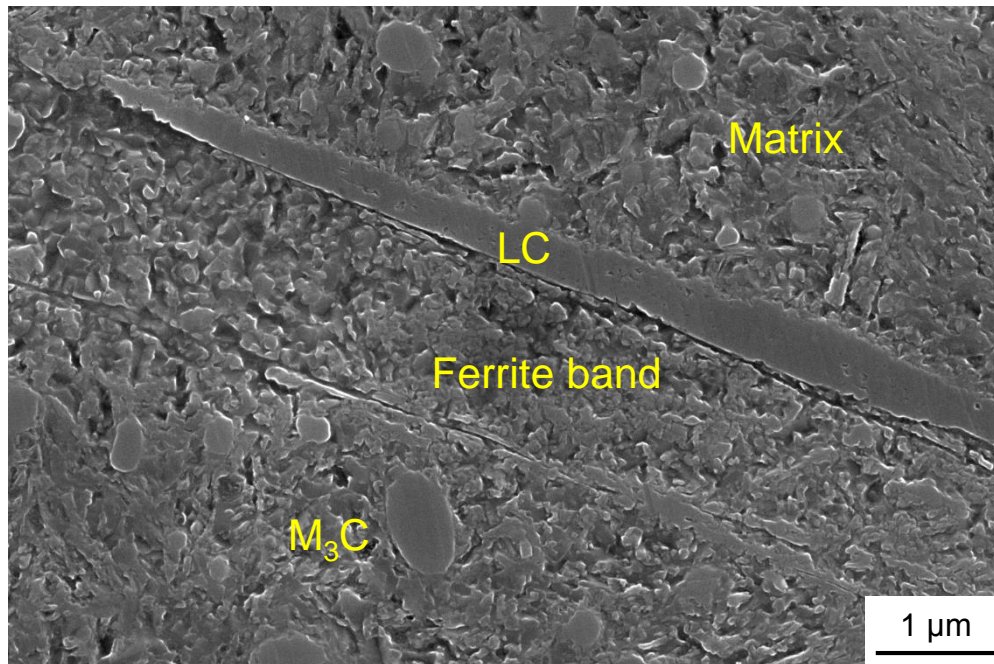
Characterisation – DERs

Atom probe tomography (APT) on a DER

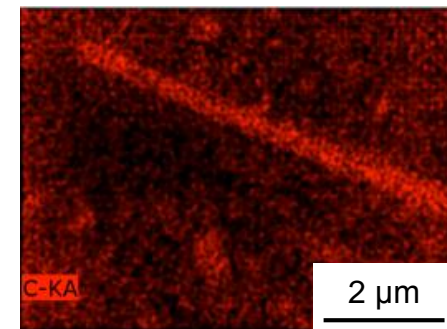
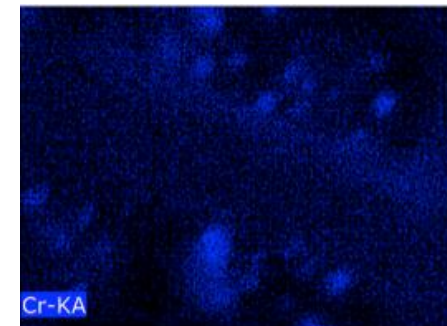
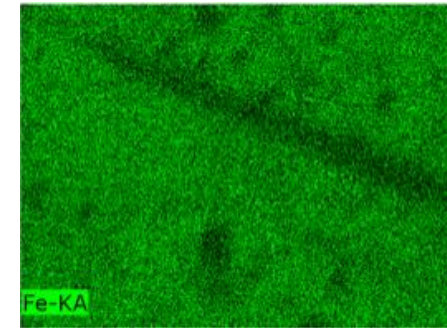
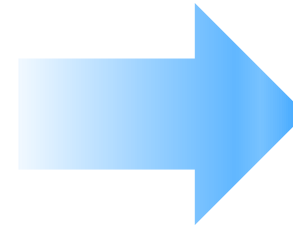


➤ Strong evidence of carbon segregation to pre-existing precipitates.

Characterisation – WEBs



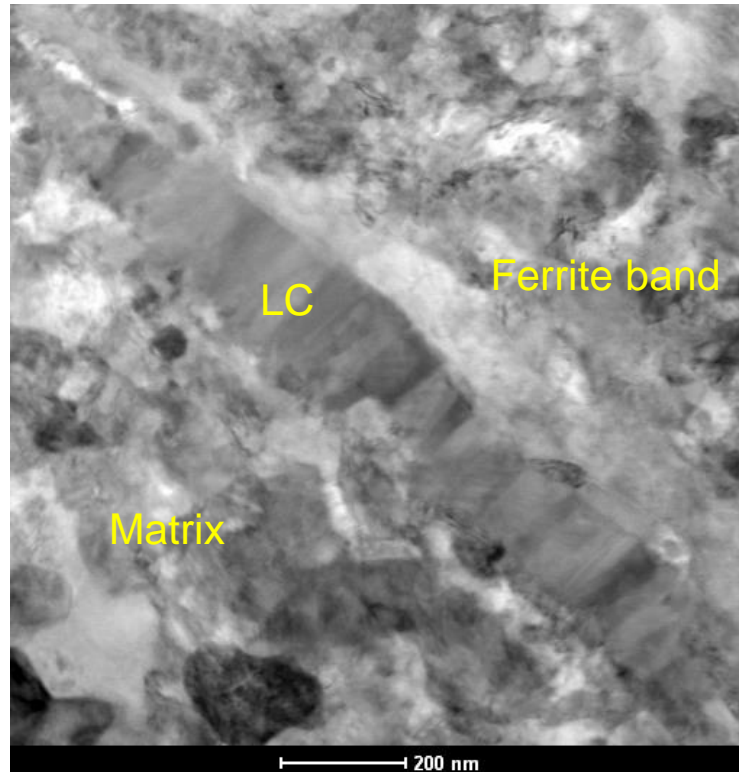
Mapping of elements using energy-dispersive X-ray spectroscopy (EDX)



- C enrichment is found in both the LC and the M_3C carbides.
- Fe depletion is found in both the LC and the M_3C carbides.
- C depletion is found inside the ferrite band compared to the surrounding matrix.
- Cr is found in the M_3C carbides only.
- **WEBs are formed due to carbon segregation to LCs.**

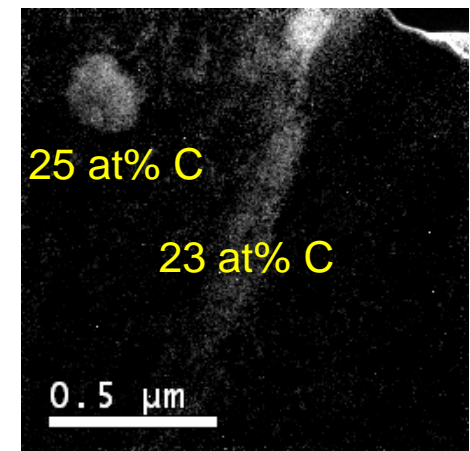
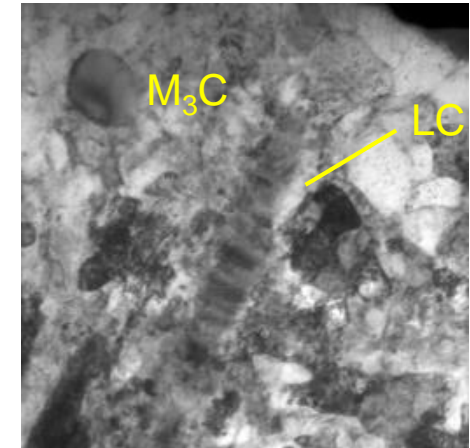
Characterisation – WEBs

Focused ion beam (FIB) and transmission electron microscopy (TEM) on a WEB



- The LC consists of numerous carbide crystallites.
- The carbon content in the LC is approximately 23 at%, close to that in cementite (25 at%).

Electron energy loss spectroscopy (EELS) on C



Summary of phenomenology and modelling strategy

Carbon redistribution

	WEAs	DERs	WEBs
Carbon-enriched zones	Dislocation cell walls	Pre-existing precipitates	Lenticular carbides
Carbon-depleted zones	Dislocation cell interiors	Matrix	Ferrite bands
Carbon migration distance	Nanometers	Hundreds of nanometers	Microns

Modelling microstructural alterations under RCF

Facts

They are form only in stress-affected regions.

They are accelerated by increasing T and/or p_0 .

They all exhibit carbon redistributions.

Martensite is a highly dislocated phase supersaturated with carbon.

Implications

They are stress-induced.

Both thermal and stress mechanisms operate during their formations.

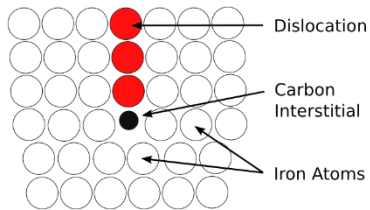
Their formations are governed by carbon migration.

The interaction between dislocations and carbon plays a vital role during their formations.

Dislocation assisted carbon migration theory

Combination of two classical theories

Cottrell atmosphere theory

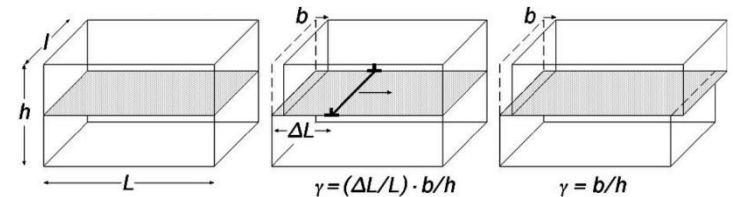


- Proposed by Cottrell and Bilby in 1949
- First observed by Chang *et al.* in 1984

$$n_C = C_{Vm} 3 \left(\frac{\pi}{2} \right)^{\frac{1}{3}} \left(\frac{AD\Delta t}{kT} \right)^{\frac{2}{3}}$$



Orowan equation



- Proposed by Orowan in 1948

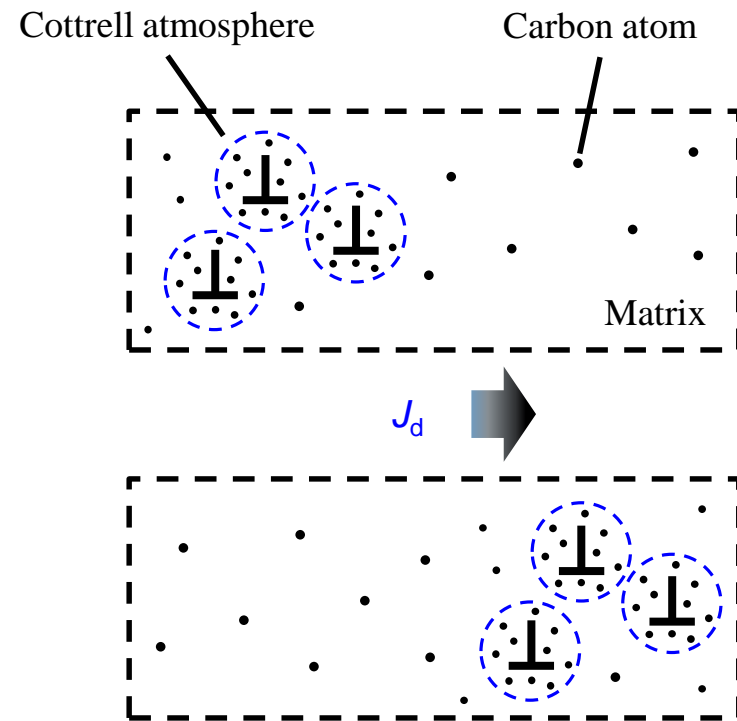
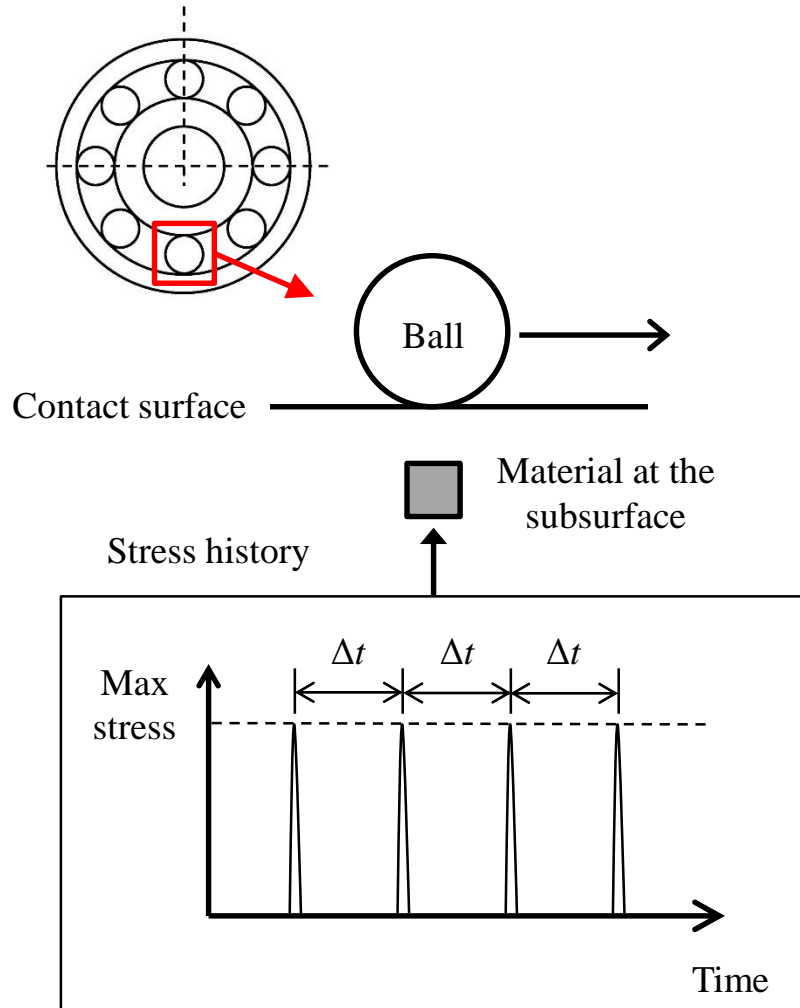
$$\dot{\gamma} = b \rho v$$

Strain rate Burgers vector Dislocation density Dislocation velocity

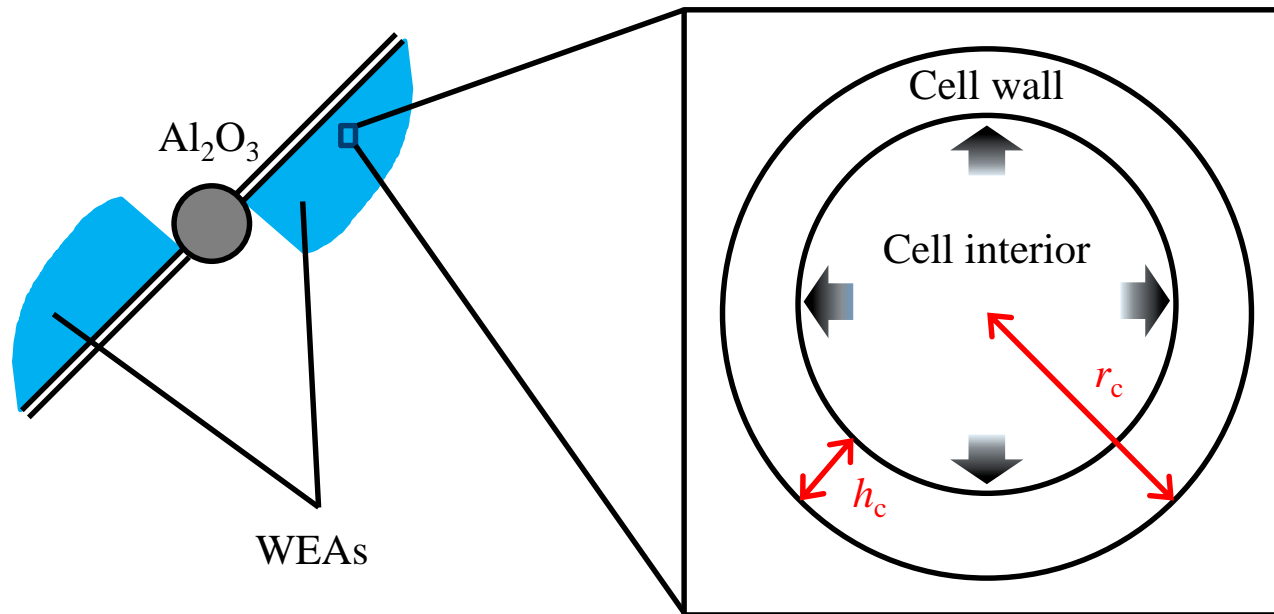


$$J_d = \frac{\Delta \dot{\gamma} \dot{N}}{b} \left[3 \left(\frac{\pi}{2} \right)^{\frac{1}{3}} \left(\frac{AD}{kT\dot{N}} \right)^{\frac{2}{3}} C_{Vm} \right]$$

Dislocation assisted carbon migration theory



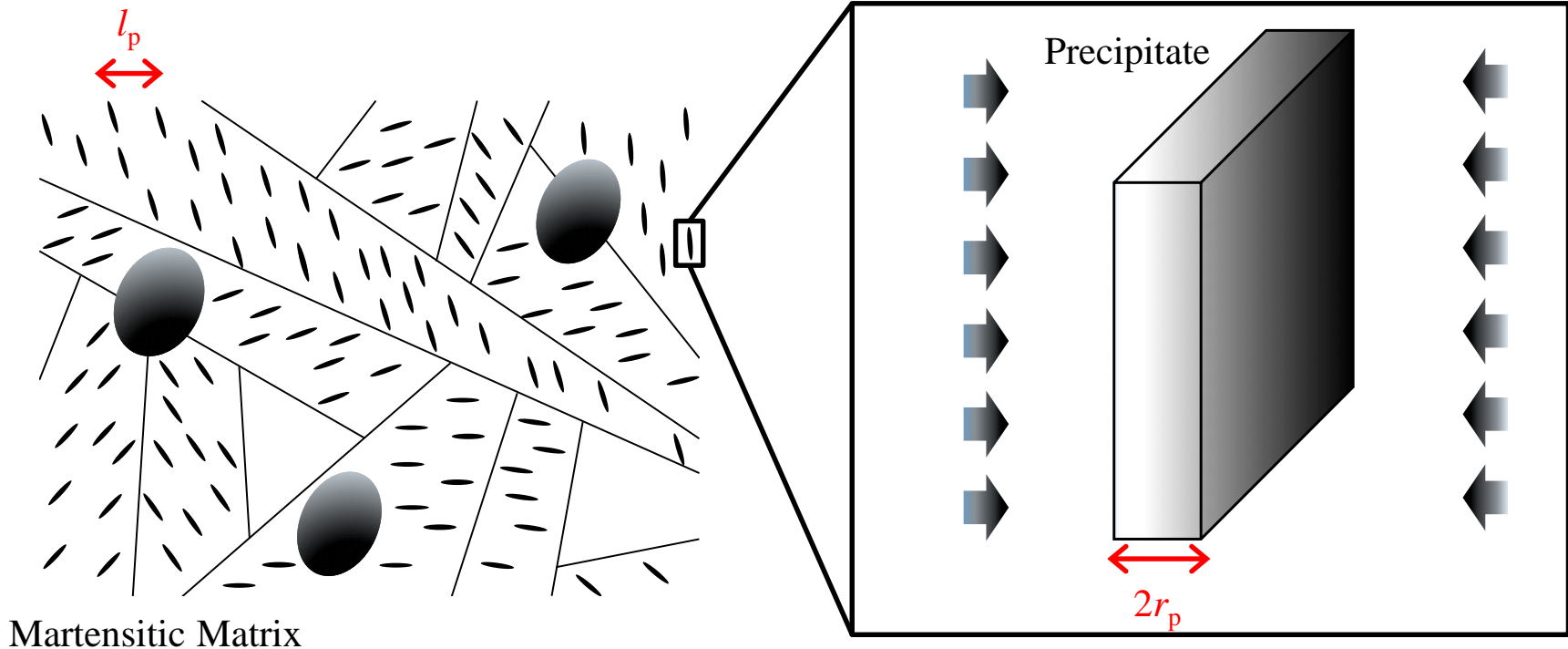
Microstructural alterations models – WEAs



$$\frac{dh_c}{dN} (C_{Vw} - C_{Vi}) \dot{N} = J_d$$

$$\frac{4}{3}\pi r_c^3 C_{V0} = \frac{4}{3}\pi (r_c - h_c)^3 C_{Vi} + \frac{4}{3}\pi [(r_c^3 - (r_c - h_c)^3) C_{Vw}]$$

Microstructural alterations models – DERs

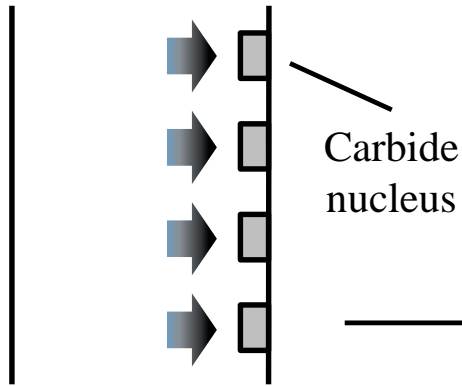


$$\frac{dr_p}{dN} (C_{Vp} - C_{Vm}) \dot{N} = J_d$$

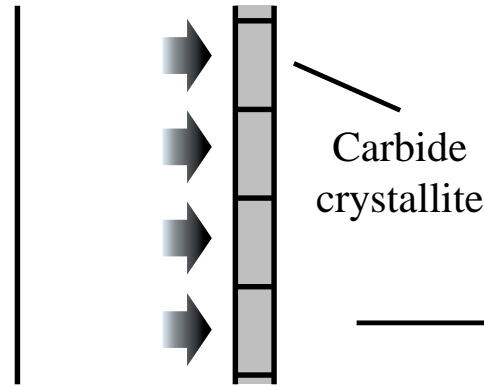
$$l_p C_{V0} = 2r_p C_{Vp} + (l_p - 2r_p) C_{Vm}$$

Microstructural alterations models – WEBs

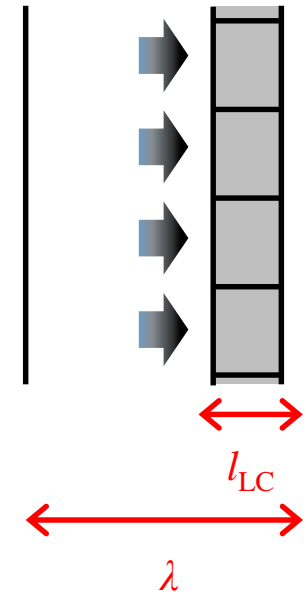
I. Carbide nucleation at ferrite band boundary



II. Coalesce of carbide crystallites to form LC



III. Carbide growth leading to LC thickening

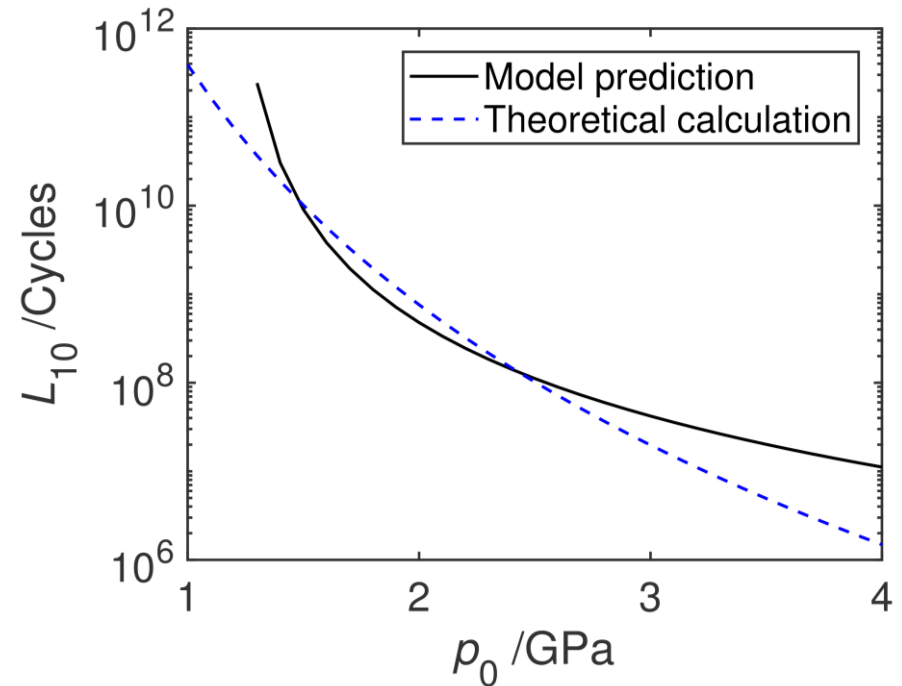
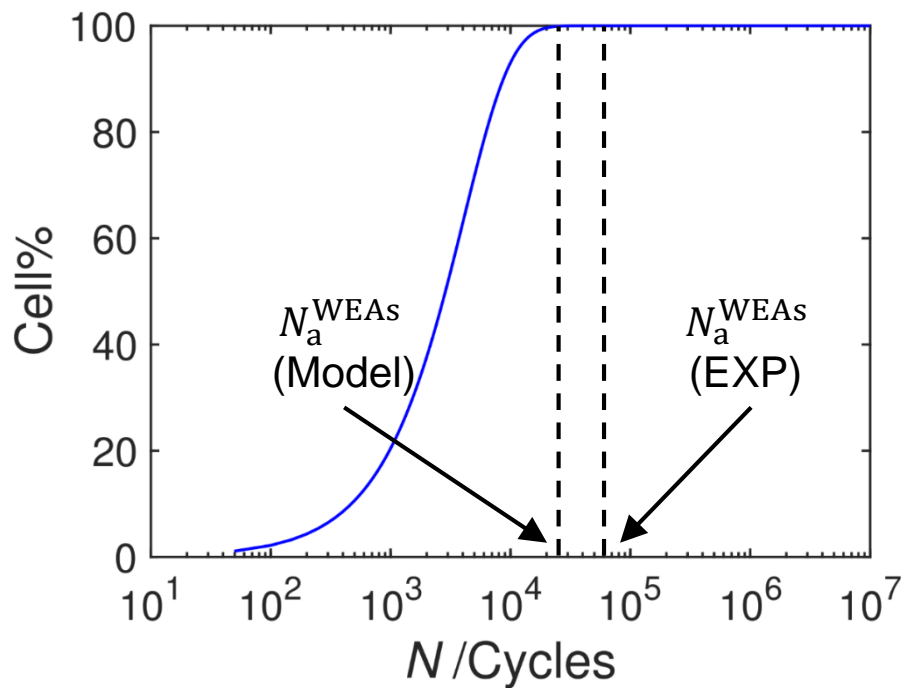


Ferrite band

$$\frac{dl_{LC}}{dN} (C_{V\theta} - C_{Vb}) \dot{N} = J_d$$

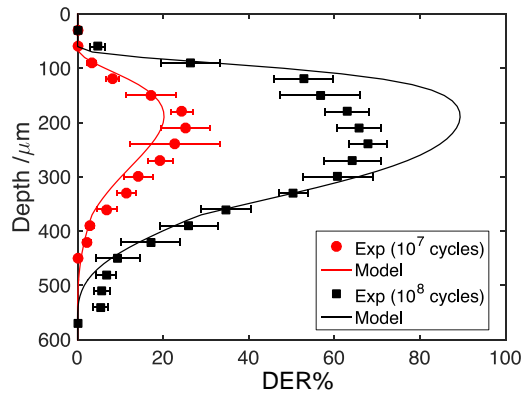
$$\lambda C_{V0} = l_{LC} C_{V\theta} + (\lambda - l_{LC}) C_{Vb}$$

Experimental verification – WEAs model

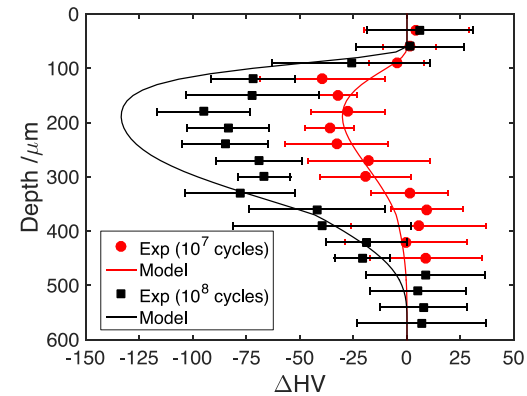


EXP and theoretical calculation: Furumura *et al.*, 1996

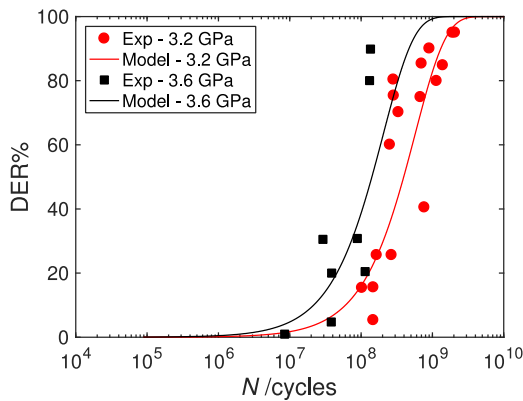
Experimental verification – DERs model



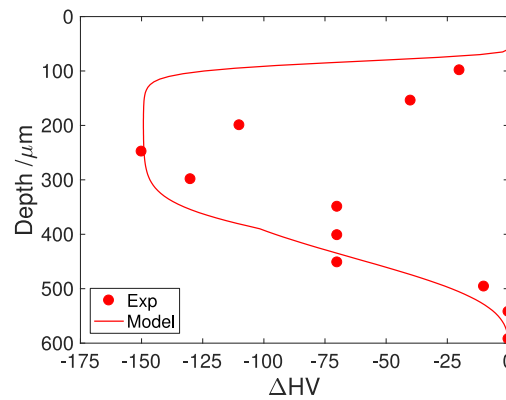
Exp: this research, 2017



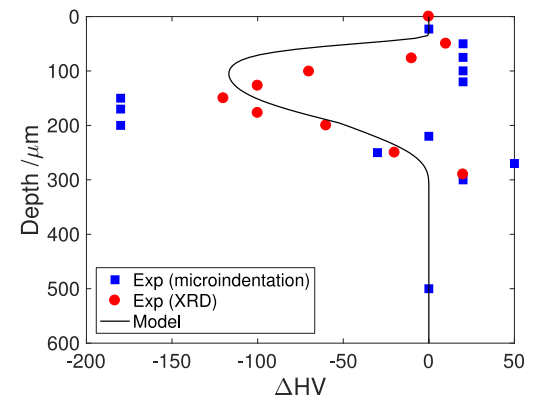
Exp: this research, 2017



Exp: Bush *et al.*, 1961

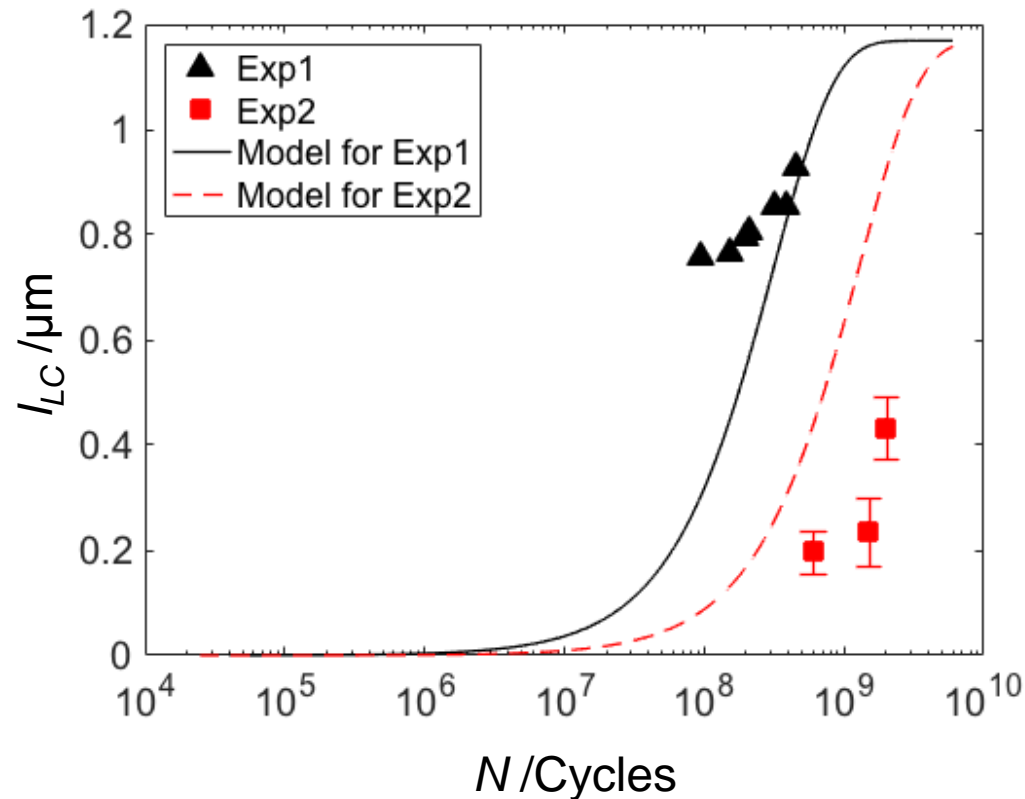


Exp: Lund, 1969



Exp: Bush *et al.*, 1961

Experimental verification – WEBs model



Exp1: Buchwald and Heckel, 1968

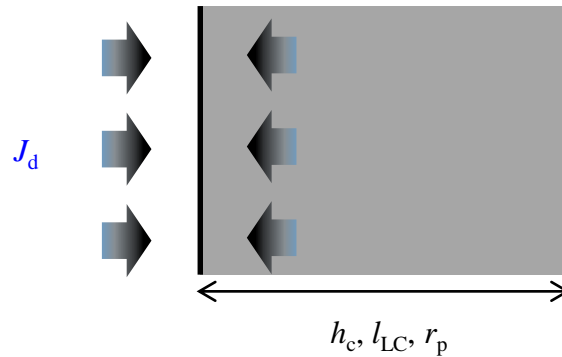
Exp2: this research, 2017

Unified theory of microstructural alterations

I (C-depleted zone)

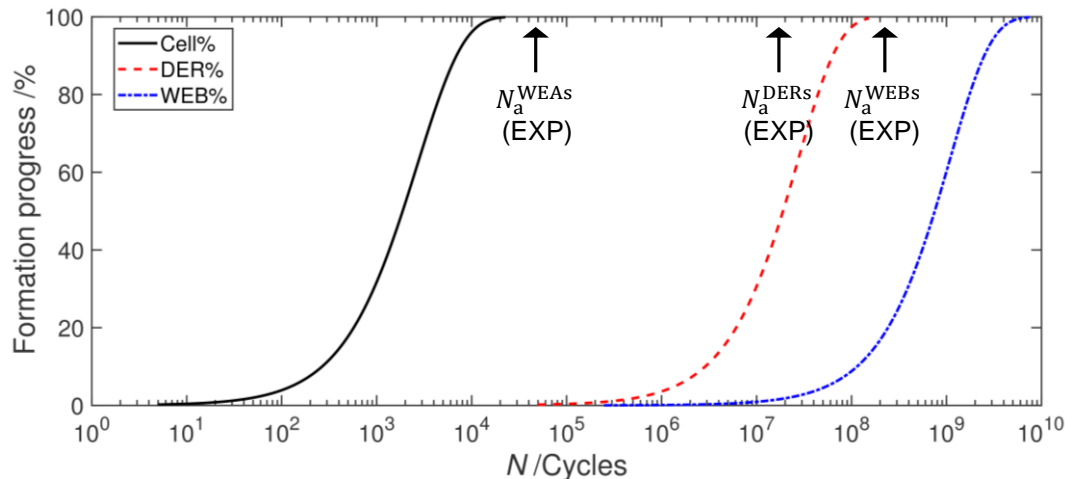
II (C-enriched zone)

Flux equilibrium



$$\frac{d(h_c, 2r_p, l_{LC})}{dN} (C_V^{II} - C_V^I) \dot{N} = J_d$$

$$V^0 C_V^0 = V^{II} C_V^{II} + (V^0 - V^{II}) C_V^I$$



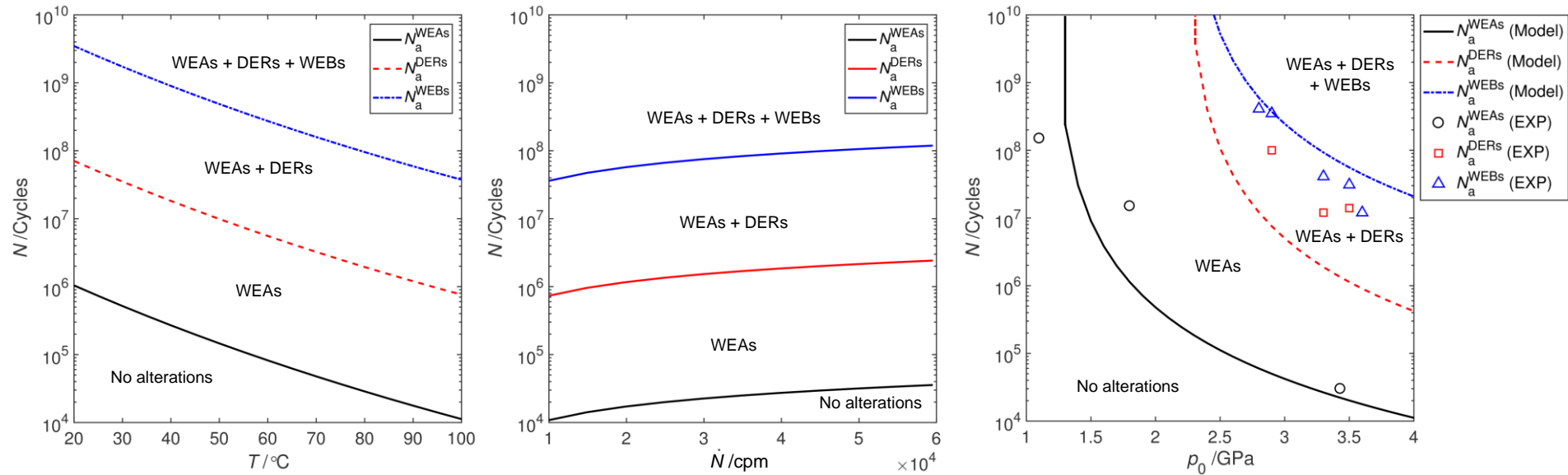
EXP: Furumura *et al.*, 1996

Summary of historical data validating the theory

Reference	Testing method	p_0 /GPa	T /°C	\dot{N} /cpm	Modelled alterations
[1]	Full-scale bearing	3.24 & 3.58	30	1×10^4	DERs
[2]	Full-scale bearing	3.27	95 – 100	4.8×10^4	WEBs
[3]	Full-scale bearing	3.4	95 – 100	4.8×10^4	WEBs
[4]	Full-scale bearing	3.3	60	3×10^4	DERs
[5]	Full-scale bearing	3.28 & 3.72	50 – 55	3×10^4	DERs & WEBs
[6]	Full-scale bearing	3.28 & 3.72	53	3×10^4	DERs & WEBs
[7]	Ball-on-rod	5.9	85	4.6×10^4	DERs & WEBs
[8]	Radial-type	4.9	60	9.4×10^2	DERs
[9]	Full-scale bearing	3.30	70	3×10^4	WEBs
[10]	Full-scale bearing	3.24	83	3×10^4	DERs
[11]	Full-scale bearing	3.43	50 – 130	3×10^4	WEAs
[12]	Full-scale bearing	1.20 – 3.43	50 – 130	3×10^4	WEAs & DERs & WEBs
[13]	Ball-on-rod	5.9	25	4.6×10^4	DERs
[13]	Ball-on-pivot	5.3	150	3.4×10^4	WEBs

- [1] J. J. Bush, W. L. Grube, G. H. Robinson, Microstructural and residual stress changes in hardened steel due to rolling contact, Transactions of the ASM 54 (1961) 390-412.
- [2] J. A. Martin, S. F. Borgese, A. D. Eberhardt, Microstructural Alterations of Rolling { Bearing Steel Undergoing Cyclic Stressing, Journal of Fluids Engineering 88 (3) (1966) 555-565.
- [3] J. Buchwald, R. W. Heckel, An analysis of microstructural changes in 52100 steel bearings during cyclic stressing, ASM Transactions Quarterly 61 (1968) 750-756.
- [4] T. Lund, Structural alterations in fatigue-tested ball-bearing steel, Jemkonter, Ann 153 (1969) 337-343.
- [5] H. Swahn, P. C. Becker, O. Vingsbo, Martensite decay during rolling contact fatigue in ball bearings, Metallurgical transactions A 7 (8) (1976) 1099-1110.
- [6] A. P. Voskamp, R. Osterlund, P. C. Becker, O. Vingsbo, Gradual changes in residual stress and microstructure during contact fatigue in ball bearings, Metals Technology 7 (1) (1980) 14-21.
- [7] T. Ochi, Y. Kusano, Change in microstructure and properties in the rolling contact fatigue of bearing steel, Nippon Steel Technical Report (80).
- [8] K. Sugino, K. Miyamoto, M. Nagumo, K. Aoki, Structural alterations of bearing steels under rolling contact fatigue, Transactions of the Iron and Steel Institute of Japan 10 (2) (1970) 98.
- [9] H. Fu, E. I. Galindo-Nava, P. E. J. Rivera-Diaz-del Castillo, Modelling and characterisation of stress-induced carbide precipitation in bearing steels under rolling contact fatigue, Acta Materialia 128 (2017) 176-187.
- [10] H. Fu, W. Song, E. I. Galindo-Nava, P. E. J. Rivera-Diaz-del Castillo, Strain-induced martensite decay in bearing steels under rolling contact fatigue: modelling and atomic-scale characterisation, Acta Materialia 139 (2017) 163-173.
- [11] K. Furumura, Y. Murakami, T. Abe, Development of long life bearing steel for full film lubrication and for poor and contaminated lubrication, Motion Control 1 (1996) 30-36.
- [12] H. Takemura, Y. Matsumoto, Y. Murakami, Development of a new life equation for ball and roller bearings, Tech. rep., SAE Technical Paper (2000).
- [13] H. Muro, N. Tsushima, Microstructural, microhardness and residual stress changes due to rolling contact, Wear 15 (5) (1970) 309-330.

Tools for bearing industry – alterations maps

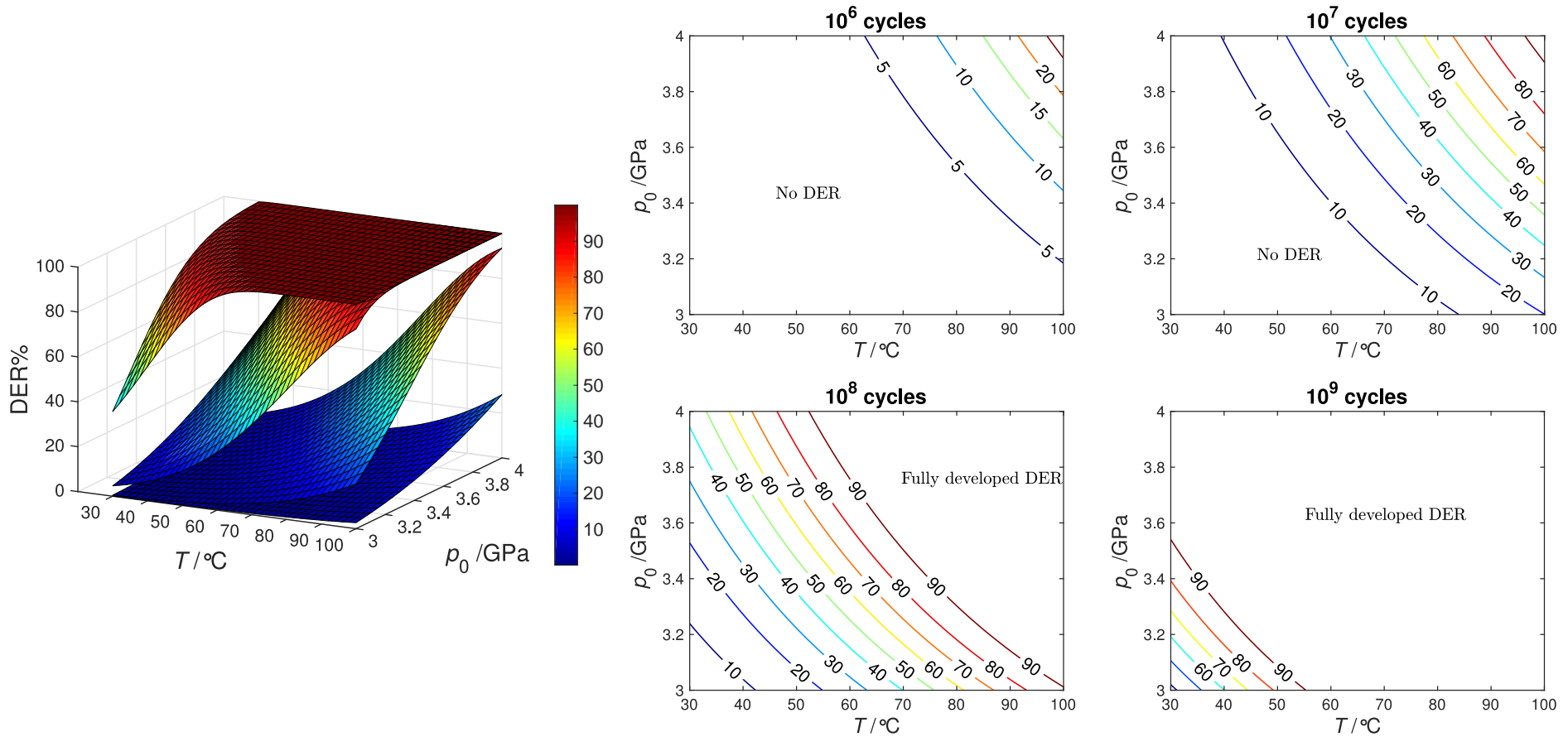


EXP: Takemura *et al.*, 2001

Before this research, microstructural alterations under RCF were studied by conducting full endurance bearing tests, which could cost up to 100,000 GBP to evaluate a new bearing type.

Now, the formation progress of any type of microstructural alterations can be directly indexed from the maps for any given RCF testing conditions. These tools are now being used by SKF.

Tools for bearing industry – DERs maps



Design of fatigue resistant bearing steels

- To avoid WEA formation – increasing carbide stability – alloying element modification & severe tempering
- To avoid DER formation – increasing steel strength – slight tempering
- To avoid WEB formation – increasing carbide stability & increasing steel strength – alloying element modification

Depending on the purpose of the bearing, a trade off must be made between different types of microstructural alterations!

- For low p_0 and low N bearings, WEA formation should be avoided by severe tempering to minimize cost.
- For low p_0 and high N bearings, WEA, DER and WEB formation should be avoided by alloying element modification.
- For high p_0 and low N bearings, DER and WEB formation should be avoided by slight tempering to minimize cost.
- For high p_0 and high N bearings, DER and WEB formation should be avoided by slight tempering with alloying element modification.

Achievements

- DERs and WEBs are characterised with advanced characterisation techniques (SEM, FIB/TEM and APT).
- A novel dislocation assisted carbon migration theory is proposed for microstructural alterations under RCF.
- The formations of three major types of microstructural alterations, WEAs, DERs and WEBs are, for the first time, quantitatively modelled.
- The suggested models are validated by experimental observations in this research.
- The suggested models are successfully applied to the reported experimental data over the past 50 years.
- Tools for bearing industry are developed, reducing the necessity of conducting expensive and time-consuming full endurance bearing tests.
- The models lead to the tailoring of novel bearing steels with outstanding fatigue resistance.

Publications

Journal articles:

1. Fu, H., E. I. Galindo-Nava, and P. E. J. Rivera-Díaz-del-Castillo. "Modelling and characterisation of stress-induced carbide precipitation in bearing steels under rolling contact fatigue." *Acta Materialia* 128 (2017): 176-187.
2. Fu, H., W. Song, E. I. Galindo-Nava, and P. E. J. Rivera-Díaz-del-Castillo. "Strain-induced martensite decay in bearing steels under rolling contact fatigue: modelling and atomic-scale characterisation." *Acta Materialia* 139 (2017): 163-173.
3. Fu, H., P. E. J. Rivera-Díaz-del-Castillo. "A unified theory for microstructural alterations in bearing steels under rolling contact fatigue" *Under preparation*.

Conference papers:

1. TMS 2018, presentation (presenter) "Modelling microstructural alterations in bearing steels under rolling contact fatigue." Accepted.
2. TMS 2018, presentation (co-author) "Crack growth under rolling contact fatigue: 3D Characterisation and Modelling." Accepted.
3. Thermec 2018, presentation (co-author) "A unified theory of microstructural changes during rolling contact fatigue." Accepted.